



Cite this: *New J. Chem.*, 2018, 42, 19917

Effect of preparation temperature on the structures and hydrodeoxygenation performance of Ni₂P/C catalysts prepared by decomposition of hypophosphites†

Xueya Dai, Hua Song, * Zijin Yan, Feng Li, Yanguang Chen, Xueqin Wang, Dandan Yuan, Jiaojing Zhang and Yuanyuan Wang

A novel method for preparing Ni₂P/C-*x* (*x* = preparation temperature, °C) catalysts in a flowing N₂ atmosphere by decomposition of hypophosphites was proposed, and the effect of preparation temperature on the hydrodeoxygenation performance of the catalysts was further investigated. X-ray diffraction (XRD), N₂-adsorption specific surface area measurements, CO uptake, and X-ray photoelectron spectroscopy (XPS) were applied. The performances of the Ni₂P/C-*x* catalysts prepared at different preparation temperatures were tested in the benzofuran hydrodeoxygenation (BF HDO) reaction. The diffraction peaks related to Ni₂P can be seen when *x* ≥ 400 °C. With increasing *x*, the Ni₂P crystallite size and CO uptake amount of the Ni₂P/C-*x* catalysts increased, and the amount of phosphorous decreased. The BF conversion and yield of total O-free products over the Ni₂P/C-*x* catalysts increased with increasing preparation temperature. The Ni₂P/C-550 catalyst showed a BF HDO conversion of 91.6% and a yield of total O-free products of 70.2% under the reaction conditions of 300 °C, 3.0 MPa, a H₂/oil ratio of 500 (V/V), and a weight hourly space velocity (WHSV) of 4.0 h⁻¹.

Received 11th September 2018,
Accepted 22nd October 2018

DOI: 10.1039/c8nj04628j

rsc.li/njc

1. Introduction

Biomass, the most abundant and inexpensive renewable resource, has been attracting much attention. Bio-oil produced from biomass is a potential liquid fuel to replace fossil fuels in the current conversion system and energy production. However, bio-oil contains a high fraction of oxygenated compounds, which degrade the physical and chemical stability of bio-oil. The oxygen in bio-oil can be removed by catalytic hydrodeoxygenation (HDO). Therefore, the development of highly active HDO catalysts has received much attention.^{1–3}

A series of catalysts has been studied for HDO, such as conventional sulfide catalysts, noble metal catalysts, and transition metal phosphides. Sulfide catalysts have a drawback in that they require the addition of environmentally unfriendly sulfur to maintain their catalytic activity. Noble metal catalysts are too expensive for industrial applications. The transition metal phosphides, such as Ni₂P, WP, Co₂P, MoP and NiMoP, have attracted much attention due to their widespread availability,

cheap cost and high hydrotreating activity.⁴ Among them, Ni₂P with unique physical and chemical properties is the most promising catalyst.⁵

Several preparation methods of Ni₂P catalysts have been reported in the literature. Temperature programmed reduction (TPR) of a nickel metal salt together with a phosphate under flowing hydrogen is a traditional method for the preparation of Ni₂P, which has the disadvantage of requiring high treatment temperatures (> 650 °C).⁶ Besides the TPR method, some new methods have been proposed for the preparation of Ni₂P, such as solution-phase reactions,⁷ reduction of nickel dihydrogenphosphite,⁸ thermal decomposition of nickel thiophosphate (NiPS₃),⁹ thermal decomposition of trioctylphosphine (TOP) together with metal salt precursors,^{10,11} plasma methods,¹² and thermal decomposition of hypophosphites or dihydrogenphosphite in an inert atmosphere. Of all these preparation methods, the thermal decomposition of hypophosphites or dihydrogenphosphite in an inert atmosphere is particularly noteworthy with the advantage of a lower preparation temperature and no need for H₂.¹³ Song *et al.*¹⁴ prepared bulk and supported Ni₂P/SiO₂ catalysts using NaH₂PO₃ and NiCl₂·6H₂O as precursors with the initial molar ratio of H₂PO₃⁻/Ni²⁺ = 5 in flowing N₂ at 250 °C, in which dihydrogenphosphite released PH₃ when it decomposed. PH₃ can reduce NiCl₂·6H₂O to form Ni₂P. They found that too low or too high a treatment

Provincial Key Laboratory of Oil & Gas Chemical Technology, College of Chemistry & Chemical Engineering, Northeast Petroleum University, Daqing 163318, Heilongjiang, China. E-mail: songhua2004@sina.com; Fax: +86 0459 6503167; Tel: +86 0459 6503167

† Electronic supplementary information (ESI) available. See DOI: 10.1039/c8nj04628j

temperature and a low $\text{H}_2\text{PO}_3^-/\text{Ni}^{2+}$ molar ratio would lead to the formation of Ni_{12}P_5 besides the main phase of Ni_2P . The conversion of dibenzothiophene (DBT) hydrodesulfurization (HDS) over $\text{Ni}_2\text{P}/\text{SiO}_2$ was found to be about 93% and 100% at 340 °C and 360 °C, respectively. Guan *et al.*¹⁵ prepared bulk Ni_2P , $\text{Ni}_2\text{P}/\text{Al}_2\text{O}_3$ and $\text{Ni}_2\text{P}/\text{MCM-41}$ by heating NiO (calcined from $\text{Ni}(\text{NO}_3)_2$) together with NaH_2PO_2 in a static Ar atmosphere. The prepared $\text{Ni}_2\text{P}/\text{Al}_2\text{O}_3$ and $\text{Ni}_2\text{P}/\text{MCM-41}$ catalysts showed a DBT HDS activity of 84% and 100% at 330 °C, respectively. Similarly, Bowker *et al.*¹⁶ prepared a $\text{Ru}_2\text{P}/\text{SiO}_2$ catalyst, and they used hypophosphite as a reductant to reduce Ru^{3+} . The prepared $\text{Ru}_2\text{P}/\text{SiO}_2$ catalyst had a furan HDO activity of 12 390 nmol furan $\text{g}^{-1} \text{s}^{-1}$ at 400 °C. From the above, the thermal decomposition of hypophosphites or dihydrogenphosphite is a promising method for the preparation of Ni_2P due to its lower preparation temperature and no need for H_2 . However, most of the prepared Ni_2P catalysts were applied in the HDS reaction and seldom used in the HDO reaction.

The difference in terms of Ni sources can affect the structure and activity of the Ni_2P catalyst. Nickel acetate ($\text{Ni}(\text{CH}_3\text{COO})_2 \cdot 4\text{H}_2\text{O}$) is a potential Ni source for high surface area and uniform particles of catalysts.¹⁷ Dharmaraj *et al.*¹⁷ prepared NiO particles with uniform size and good dispersion using nickel acetate as a Ni source. They found that the nickel acetate coordinated with poly(vinyl acetate) could prevent the aggregation of NiO during heat treatment. When $\text{Ni}(\text{CH}_3\text{COO})_2 \cdot 4\text{H}_2\text{O}$ is heated in an inert atmosphere, CO produced from the thermal decomposition of the acetate group reduces the Ni^{2+} state to Ni.^{18,19} Inspired by this, a novel method to prepare a Ni_2P catalyst using $\text{Ni}(\text{CH}_3\text{COO})_2 \cdot 4\text{H}_2\text{O}$ as the Ni source in an inert atmosphere by the thermal decomposition of hypophosphite is proposed in this study. Besides the influence of Ni sources, the preparation temperature is another important condition to modulate the structure and activity of the catalyst. Wang *et al.*²⁰ investigated the effect of calcination and reduction temperatures on unsupported Ni_2P catalysts. The results indicated that the highest Ni_2P surface area could be obtained from a precursor calcined at 500 °C and reduced in H_2 at 650 °C, and the smallest Ni_2P crystallite size was obtained at 500 °C. Chen *et al.*²¹ revealed the influence of the reduction temperature (400–550 °C) for $\text{NiMoO}_3\text{-x}/\text{SAPO-11}$ catalysts on the HDO performance of methyl laurate, involving the aspects of deoxygenation activity, isomerization selectivity and deoxygenation pathway. The $\text{NiMo}_3\text{-x}/\text{SAPO-11}$ catalyst reduced at 400 °C exhibited a low deoxygenation activity with the highest isomerization selectivity. However, the effect of preparation temperature on the supported Ni_2P catalysts using $\text{Ni}(\text{CH}_3\text{COO})_2 \cdot 4\text{H}_2\text{O}$ as a Ni source in an inert atmosphere by the thermal decomposition of hypophosphite has not been thoroughly studied yet.

Activated carbon (C) has large average pore diameters, and large surface areas and pore volumes, and it is an economical support for various catalysts.^{22,23} Using C as a support, a series of $\text{Ni}_2\text{P}/\text{C}$ catalysts were prepared from $\text{Ni}(\text{CH}_3\text{COO})_2 \cdot 4\text{H}_2\text{O}$ and ammonium hypophosphite ($\text{NH}_4\text{H}_2\text{PO}_2$) at different temperatures in a flowing N_2 atmosphere. The effect of temperature on the textural characterization and benzofuran (BF) HDO activity

was investigated. Furthermore, a BF HDO reaction route was proposed to interpret the catalytic behavior of the catalyst.

2. Experimental methods

2.1. Preparation of bulk and supported nickel phosphide

In order to determine the proper initial P/Ni molar ratio, bulk nickel phosphide catalysts with different initial P/Ni molar ratios (P/Ni = 2, 3, 4, and 5) were synthesized by dissolving $\text{NH}_4\text{H}_2\text{PO}_2$ and $\text{Ni}(\text{CH}_3\text{COO})_2 \cdot 4\text{H}_2\text{O}$ in deionized water. In a typical experiment (P/Ni = 2), 8.04 mmol of $\text{Ni}(\text{CH}_3\text{COO})_2 \cdot 4\text{H}_2\text{O}$ and 16.08 mmol of $\text{NH}_4\text{H}_2\text{PO}_2$ were respectively dissolved in 20 mL of deionized water at room temperature to form uniform solutions. The solutions were evaporated at 60 °C for 12 h until they were dehydrated. The obtained solids were then ground using a mortar and pestle to form ready-to-use precursors. The precursors (0.3 g) were placed in a fixed-bed reactor, heated to 400 °C, at a rate of 3 °C min^{-1} in a flow of N_2 (30 mL min^{-1}), held for 2 h, then naturally cooled to 100 °C and held for another 1 h in flowing air (30 mL min^{-1}), instead of being passivated with an O_2/N_2 mixture. In this way, the reactivation step of the catalyst under high temperature in a H_2 flow prior to reaction, like the conventional method, can be omitted.^{24,25}

To make the $\text{Ni}_2\text{P}/\text{C-x}$ catalysts, a calculated C (activated carbon, Xuan Cheng Jing Rui New Material Co., Ltd, 16/20 mesh, washed with deionized water and dried at 100 °C for 10 h) support was added to the solution of $\text{NH}_4\text{H}_2\text{PO}_2$ and $\text{Ni}(\text{CH}_3\text{COO})_2 \cdot 4\text{H}_2\text{O}$ (initial P/Ni molar ratio = 4, Ni = 10 wt%). In a typical experiment, 3.38 mmol of $\text{Ni}(\text{CH}_3\text{COO})_2 \cdot 4\text{H}_2\text{O}$ and 13.61 mmol of $\text{NH}_4\text{H}_2\text{PO}_2$ were dissolved in 20 mL of deionized water at room temperature to form a uniform solution. 2.0 g of the C support was wet-impregnated with the above solution for 12 h. The subsequent steps and conditions are the same as those for synthesizing bulk nickel phosphide catalysts. The precursor (0.3 g) was placed in a fixed-bed reactor and heated to 350 °C, 400 °C, 450 °C, 500 °C and 550 °C, respectively. The catalysts obtained were named as $\text{Ni}_2\text{P}/\text{C-x}$, where the x was defined as the thermal treatment temperature (°C).

2.2. Characterization

X-ray diffraction (XRD) analysis was carried out on a D/max-2200PC-X-ray diffractometer using Cu K α radiation, with the scan range from 10 to 80° at a rate of 10° min^{-1} . All the samples were air-modified catalysts. The typical physico-chemical property of the catalysts was analyzed by the BET method using a micromeritics adsorption Tristar II 3020 instrument. All the samples were treated at 200 °C under vacuum conditions with the pressure of 6 mmHg. The adsorption isotherms for nitrogen were measured at –196 °C. CO uptake measurement was performed in a Micromeritics ASAP 2010 apparatus. Typically, 0.2 g of catalyst was loaded in a quartz reactor and treated in a continuous He flow (30 mL min^{-1}) for 30 min at 200 °C to remove moisture, then naturally cooled down to room temperature to achieve an adsorbate-free state by flushing for 30 min. After pre-treatment, pulses of CO (1 mL) were injected into the flow of

He (30 mL min⁻¹), which were repeatedly injected until the response from the detector showed no further CO uptake after consecutive injections. The CO uptake was calculated by measuring the decrease in peak areas due to adsorption. The X-ray photoelectron spectroscopy (XPS) spectrum was acquired using an ESCALAB MKII spectrometer under vacuum. XPS measurement was performed with Mg radiation ($E = 1253.6$ eV) and a hemi-spherical analyzer operating at a fixed pass energy of 40 eV. The recorded photoelectron binding energy was referenced against the C 1s contamination line at 284.8 eV. All the samples were air modified catalysts.

2.3. Catalytic activity test

The reaction was performed in a flowing high-pressure fixed-bed stainless steel catalytic reactor (0.8 cm in diameter and 40 cm in length), using a feed consisting of a decalin solution of BF (2 wt%). The conditions for the HDO reaction were 300 °C, 3.0 MPa, weight hourly space velocity (WHSV) = 4.0 h⁻¹, and a hydrogen/liquid ratio of 500 (V/V). The feed and reaction product were analyzed by flame ionization detector (FID) gas chromatography (Shimadzu GC-14C) equipped with a capillary column (PH-1, 60 m × 0.25 mm). The temperature program was heating at a rate of 20 °C min⁻¹ from 70 °C to 250 °C, then holding at 250 °C for 1 min.

The conversion of BF (X_{BF}), the selectivities and yields of O-free products, and the selectivity (S_i) were defined as follows, respectively:

$$X_{BF} = \left(1 - \frac{n_{BF}}{n_{BF,0}}\right) \times 100\% \quad (1)$$

$$\text{Selectivities}_{O\text{-free}} = \frac{\text{O-free product}}{\text{all product}} \times 100\% \quad (2)$$

$$\text{Yields}_{O\text{-free}} = \text{Conversion} \times \text{Selectivities}_{O\text{-free}} \times 100\% \quad (3)$$

$$S_i = \frac{n_i}{\sum n_i} \times 100\% \quad (4)$$

where $n_{BF,0}$ and n_{BF} are the moles of BF in the feed and product, respectively, and n_i is the moles of product i .

3. Results and discussion

3.1. XRD patterns of the Ni₂P/C- x catalysts

Fig. S1 (ESI[†]) shows the XRD patterns of the bulk samples with different initial P/Ni molar ratios. All samples showed Ni₂P phase peaks at $2\theta = 40.6^\circ$, 44.5° , 47.1° and 54.1° (PDF: 03-0953). However, the pure Ni₂P phase could only be obtained for the catalysts with an initial P/Ni ratio higher than 4.

XRD patterns were used to identify the crystalline phases. Fig. 1 shows the XRD patterns of the C support and Ni₂P/C- x catalysts. For the C support, the broad diffraction peaks located at $2\theta = 23.9^\circ$ and 42.7° were due to the amorphous nature of the micropore structure.²⁶ For Ni-P/C-350, the diffraction peaks related to Ni₂P did not appear. With increasing preparation temperature, the peaks at $2\theta = 40.6^\circ$, 44.5° , 47.1° and 54.1°

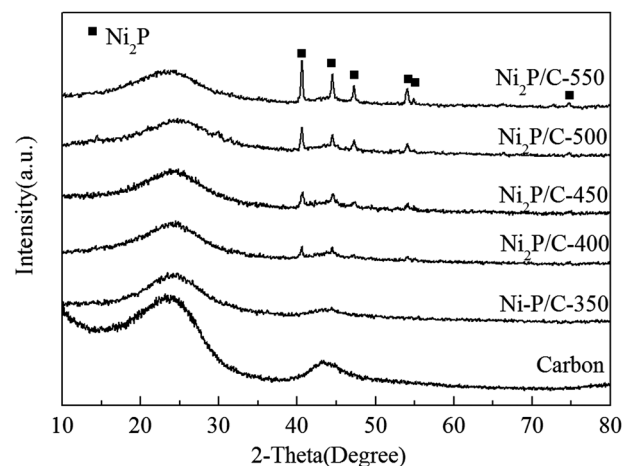


Fig. 1 XRD patterns of Ni₂P/C- x catalysts.

Table 1 Properties of C support and Ni₂P/C- x catalysts

Sample	S_{BET} (m ² g ⁻¹)	V_p (cm ³ g ⁻¹)	D^a (nm)	d_{XRD}^b (nm)	CO uptake (μmol g ⁻¹)	Yields of O-free product (%)
C support	907	0.31	1.37	—	—	—
Ni ₂ P/C-400	218	0.14	2.57	18.5	32	62.9
Ni ₂ P/C-450	221	0.15	2.71	18.9	33	66.0
Ni ₂ P/C-500	263	0.17	2.59	20.0	35	67.0
Ni ₂ P/C-550	284	0.17	2.39	25.6	36	70.2

^a D : pore diameter, $D = 4V_{BJH}/S_{BET}$. ^b d_{XRD} : calculated from the Scherrer equation based on Ni₂P {1 1 1}.

(PDF: 03-0953), ascribed to the Ni₂P phase, can be clearly seen. No other phase related to Ni or P could be seen, indicating that the active phase was mainly Ni₂P.

The average size of the Ni₂P crystallites estimated by the Scherrer equation is shown in column 5 of Table 1. The average size of the Ni₂P crystallites increased from 18.5 nm (Ni₂P/C-400) to 20.0 nm (Ni₂P/C-500) with increasing preparation temperature from 400 °C to 500 °C. But, when increasing the temperature from 500 °C to 550 °C (25.6 nm), the average size of the Ni₂P crystallites showed an increase of 5.6 nm, which is large. Similar results were reported by Wang *et al.*,²⁰ in which the crystallite size of Ni₂P increased gradually from 9 to 20 nm with the reduction temperature increasing from 500 to 650 °C.

3.2. N₂ adsorption of Ni₂P/C- x catalysts

Fig. 2 shows the N₂ adsorption-desorption isotherms for the C support and Ni₂P/C- x catalysts. As can be seen from Fig. 2, the samples displayed a type IV isotherm and a standard H4 type hysteresis loop according to the IUPAC classification, showing the presence of some mesopores. Table 1 shows the textural properties of the support and catalysts. The surface area and pore volume of the C support were 907 m² g⁻¹ and 0.31 cm³ g⁻¹, respectively. The surface area and pore volume of the Ni₂P/C- x catalysts decreased significantly as compared to those of the C support, which was due to the blockage of pores by loading the nickel phosphide phase. The Ni₂P/C-400 catalyst showed a surface area of 218 m² g⁻¹. With the increase of

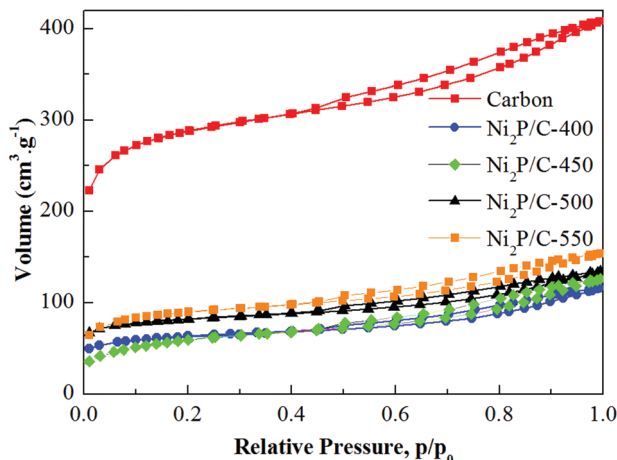


Fig. 2 Nitrogen adsorption/desorption isotherms of the C support and Ni₂P/C-*x* catalysts.

temperature, the surface area increased. The surface area of the Ni₂P/C-500 catalyst increased to 263 m² g⁻¹. But, when increasing the temperature from 500 °C to 550 °C, the increase of surface area was little.

The results indicated that a higher preparation temperature is beneficial to obtain a large surface area, which coincides with those of the previously published studies.¹³ This can be attributed to a decrease in the enrichment of phosphorus on the surface of the catalysts with increasing preparation temperature. This will be further discussed in Section 3.4 XPS analysis.

3.3. CO uptake of Ni₂P/C-*x* catalysts

The CO uptakes of the catalysts are listed in column 6 of Table 1. The CO uptake data were measured five times and the listed data are the average values. The average error was less than 5.5%. According to the literature,^{27,28} the CO molecules are mainly adsorbed at Ni sites; therefore, the amount of CO uptake can reflect the amount of exposed Ni sites on the

catalysts. As can be seen from Table 1, the CO uptake of Ni₂P/C-400 was 32 μmol g⁻¹, which is low compared to those of the other catalysts prepared at higher temperatures. The low CO uptake of Ni₂P/C-400 was possibly due to the enrichment of phosphate species on the surface (see XPS analysis) at a lower preparation temperature. With increasing preparation temperature, the CO uptake increased, showing more active Ni sites could be exposed on the surface of the catalysts. This is because a higher preparation temperature is beneficial to suppress the enrichment of phosphate species on the surface (see XPS analysis).

3.4. XPS spectra of the Ni₂P/C-*x* catalysts

The XPS spectra were analysed to gain further insight into the valence states of the active components and the surface composition of the catalysts. Fig. 3 shows the XPS spectra for the Ni 2p and P 2p lines of the Ni₂P/C-400 and Ni₂P/C-550 catalysts. As shown in Fig. 3(a), the peaks centered at 853.5 eV can be assigned to Ni^{δ+} (0 < δ < 2) in Ni₂P. The peaks centered at 856.3–856.4 eV correspond to the possible interaction of Ni²⁺ ions with phosphate ions, as a consequence of a superficial passivation, along with the broad shake-up peak at approximately 6.0 eV higher than that of the Ni²⁺ species.²⁹ In Fig. 3(b), the peaks centered at 130.2–130.3 eV can be assigned to P^{δ-} (0 < δ < 1) in the Ni₂P phase and the peak at 134.5–134.6 eV can be assigned to P⁵⁺ due to the superficial oxidation.³⁰

The superficial atomic ratios of P/Ni obtained from XPS are listed in column 7 of Table 2. The initial P/Ni molar ratio of Ni₂P/C-*x* was 4. However, the data from XPS analysis showed that Ni₂P/C-400 and Ni₂P/C-550 exhibited lower P/Ni ratios than 4, which may be because of the release of PH₃ during the preparation. But, the P/Ni ratios of Ni₂P/C-*x* were still higher than the theoretical P/Ni ratio of 0.5 of the Ni₂P phase, which may be due to the enrichment of phosphorous on the surface. The superficial P/Ni ratio of Ni₂P/C-400 was 3.07, and that of Ni₂P/C-550 decreased to 2.15. This indicated that a higher preparation temperature was beneficial to suppress the enrichment

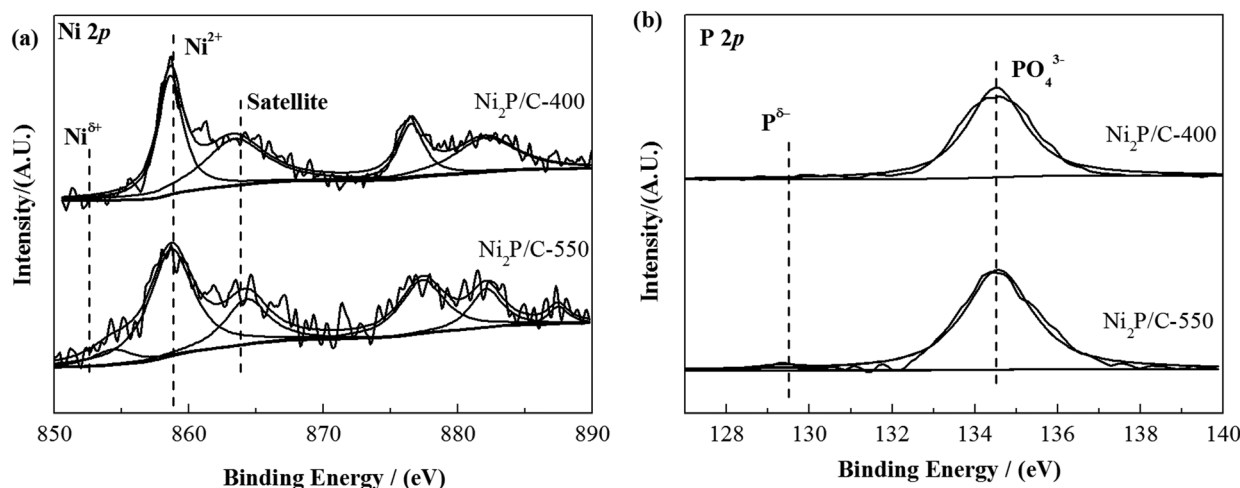


Fig. 3 XPS patterns in the Ni(2p) and P(2p) regions of the Ni₂P/C-*x* catalysts. (a) Ni 2p core level spectra and (b) P 2p core level spectra.

Table 2 Proportion of each species from the Ni(2p) and P(2p) spectra obtained by XPS analysis

Sample	Binding energy (eV)					Superficial atomic ratio P/Ni
	Ni 2p _{3/2}			P 2p		
	Ni ⁰⁺	Ni ²⁺	Satellite	P ^{δ-}	P ⁵⁺	
Ni ₂ P/C-400	853.5	856.3	861.1	130.3	134.6	3.07
Ni ₂ P/C-550	853.5	856.4	861.3	130.2	134.5	2.15

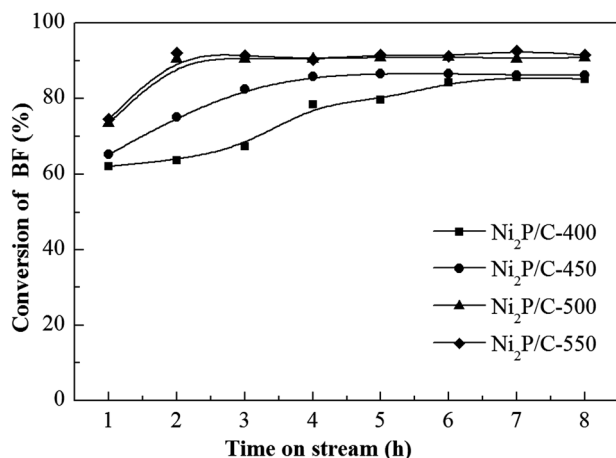


Fig. 4 Conversion of BF HDO over Ni₂P/C-*x* catalysts.

of phosphorous, possibly related with the release of a larger amount of PH₃ at higher temperature.

3.5. Catalytic results and reaction pathways

Fig. 4 depicts the reaction of BF HDO over the Ni₂P/C-*x* catalysts as a function of reaction time. As shown in Fig. 4, the BF conversion gradually increased and then remained stable with time. The improved catalytic activities within the initial time indicated that an intermediate phase, which was more active than Ni₂P,^{31,32} was formed. Korányi *et al.*²⁹ reported that a superficial phosphosulfide with a stoichiometry represented by NiP_{*x*}S_{*y*} is the real active phase of the HDS reaction. Similar to the HDS reaction, the HDO conversion increasing with time-on-stream may be caused by the formation of a more active NiP_{*x*}O_{*y*} phase.³³ The surface of the Ni₂P/C catalysts was modified in air, however, the real active NiP_{*x*}O_{*y*} phase for HDO could not form completely at the initial stage. The gradually increasing conversion of BF with time-on-stream verifies the formation of more and more active NiP_{*x*}O_{*y*} phase. A similar result was also observed in our previous experiment³³ wherein the HDO activities over Ni₂P/SBA-15 catalysts gradually enhanced and remained stable with time-on-stream.

The BF conversion over the Ni₂P/C catalysts increased from 85.2% (Ni₂P/C-400) to 90.8% (Ni₂P/C-500) when the preparation temperature increased from 400 °C to 500 °C. However, when increasing the temperature from 500 °C to 550 °C, the BF conversion reached 91.6%, an increase of 0.8%. This indicates that a higher catalyst preparation temperature was beneficial for BF conversion, which was possibly because more active Ni₂P

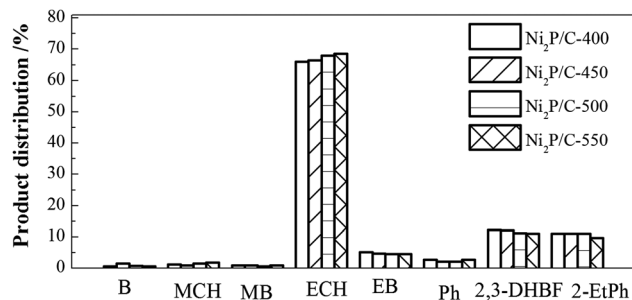


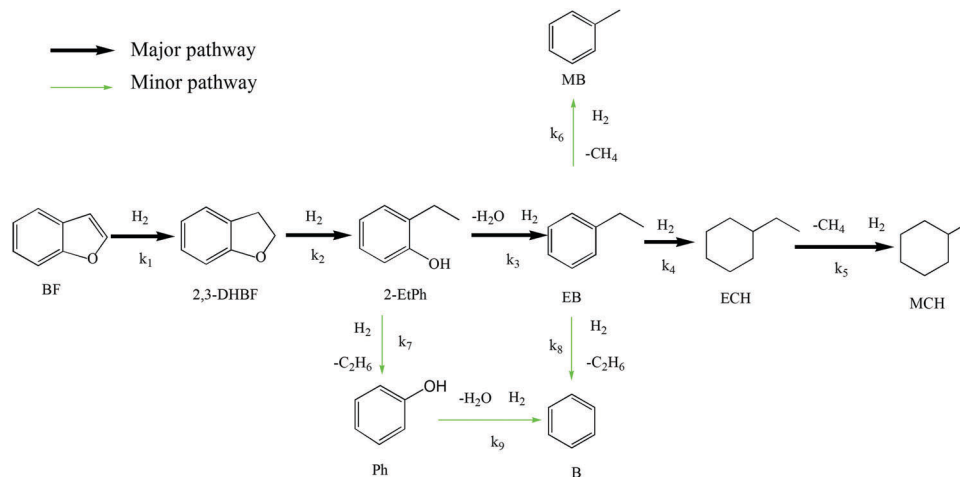
Fig. 5 Product selectivities of BF HDO over Ni₂P/C-*x* catalysts.

phase (CO analysis) was exposed on the surface of catalysts prepared at higher temperature. But, the increase of temperature has less impact on the BF conversion when the temperature was higher than 500 °C.

Fig. 5 depicts the HDO product distribution of the Ni₂P/C-*x* catalysts after 8 h. The main products detected were ethylcyclohexane (ECH), methylcyclohexane (MCH), 2-ethylphenol (2-EtPh), ethylbenzene (EB) and 2,3-dihydrobenzofuran (2,3-DHBF). Trace products observed were phenol (Ph), methylbenzene (MB) and benzene (B). The EB, ECH, MCH, MB and B were O-free products. On the basis of the product distribution and literature description,²⁵ a possible reaction route for BF HDO over Ni₂P/C-*x* catalysts is shown in Scheme 1. The first step involved the hydrogenation of the furan ring on BF, which led to the formation of 2,3-DHBF, then 2,3-DHBF was further converted into 2-EtPh by a C–O bond cleavage of the heterocyclic ring through hydrogenolysis. EB is obtained from 2-EtPh by dehydration, then converted into ECH by hydrogenation of the benzene ring, followed by demethylation of ECH to MCH. For the trace products, EB is transformed into B and MB *via* hydrogenation of the ethyl group. B can also be formed by dehydration of Ph, which is formed from 2-EtPh by demethylation.

All Ni₂P/C-*x* catalysts have a similar selectivity order, and the order of O-free product selectivity was ECH > EB > MCH > MB > B, while the order of O-containing product selectivity was 2,3-DHBF > 2-EtPh > Ph. It can be seen that the selectivity for ECH was much higher than other products over the Ni₂P/C-*x* catalysts. The selectivity for ECH over Ni₂P/C-400 was 65.8%, and that over Ni₂P/C-550 showed an increase of 2.8% and reached 68.6%. The total selectivity for O-free products over Ni₂P/C-400 was 73.8%, which over Ni₂P/C-550 was 76.6%. The slightly improved selectivities for O-free products with increasing preparation temperature showed that the effect of preparation temperature on the reaction route was not significant. At the same time, the selectivities for the main O-containing products of 2,3-DHBF and 2-EtPh over Ni₂P/C-*x* presented a slight decrease as the preparation temperature increased.

The yields of O-free compounds over Ni₂P/C-*x* catalysts after 8 h are shown in column 7 of Table 1. The yield of O-free compounds over Ni₂P/C-400 was 62.9%, which over Ni₂P/C-550 was 70.2%, showing that the higher preparation temperature is beneficial to obtain higher HDO activity.



Scheme 1 Reaction pathways for BF HDO over the Ni₂P/C-*x* catalysts.

4. Conclusions

In summary, a novel method for preparing highly active Ni₂P/C-*x* catalysts with Ni(CH₃COO)₂·4H₂O as the Ni source in a flowing N₂ atmosphere was proposed; and the effect of preparation temperature on the structures and hydrodeoxygenation performance of the Ni₂P/C-*x* catalysts was investigated. The XRD analysis showed that for Ni-P/C-350, the diffraction peaks related to Ni₂P were not apparent. With increasing preparation temperature, the Ni₂P crystallite size and CO uptake amount of the Ni₂P/C-*x* catalysts increased, and enrichment of phosphorous decreased. The BF conversion and yields of O-free products over Ni₂P/C-*x* catalysts increased first and then increased more slowly with increasing preparation temperature, and the effect of preparation temperature on reaction route was not significant. The Ni₂P/C-500 catalyst with a preparation temperature of 500 °C showed a BF HDO conversion of 90.8% and a yield of O-free compounds of 75.9%.

Conflicts of interest

There are no conflicts to declare.

Acknowledgements

The authors acknowledge the financial support from the National Natural Science Foundation of China (21276048) and Innovative scientific research projects of Innovative Practice Base for Postgraduate Training in Northeast Petroleum University (YJSCX2017-016NEPU).

References

- Z. Xiong, Y. Wang, S. S. A. Syed-Hassan, X. Hu, H. Han, S. Su, K. Xu, L. Jiang, J. Guo, E. E. S. Berthold, S. Hu and J. Xiang, *Energy Convers. Manage.*, 2018, **163**, 420.
- N. H. Zainan, S. C. Srivatsa, F. Li and S. Bhattacharya, *Fuel*, 2018, **223**, 12.
- S. Pichaikaran and A. Pandurangan, *New J. Chem.*, 2017, **41**, 16.
- M. Peroni, G. Mancino, E. Baráth, O. Y. Gutiérrez and J. A. Lercher, *Appl. Catal., B*, 2016, **180**, 301.
- Y. Deng, Y. Zhou, Y. Yao and J. Wang, *New J. Chem.*, 2013, **37**, 4083.
- W. Wang, X. Li, Z. Sun, A. Wang, Y. Liu, Y. Chen and X. Duan, *Appl. Catal., A*, 2016, **509**(1), 45.
- H. Song, M. Dai, H. L. Song, X. Wan, X. W. Xu and Z. S. Jin, *J. Mol. Catal. A: Chem.*, 2014, **385**(4), 149.
- J. A. Cecilia, A. Infantes-Molina, E. Rodríguez-Castellón and A. Jiménez-López, *J. Catal.*, 2009, **263**(1), 4.
- H. Loboué, C. Guillot-Deudon, A. F. Popa, A. Lafond, B. Rebours, C. Pichon, T. Cseri, G. Berhault and C. Geantet, *Catal. Today*, 2008, **130**(1), 63.
- A. E. Henkes and R. E. Schaak, *Chem. Mater.*, 2007, **19**, 4234.
- J. Park, B. Koo, K. Y. Yoon, Y. Hwang, M. Kang, J. G. Park and T. Hyeon, *J. Am. Chem. Soc.*, 2005, **127**, 8433.
- A. Wang, M. Qin, J. Guan, L. Wang, H. Guo, X. Li, Y. Wang, R. Prins and Y. Hu, *Angew. Chem., Int. Ed. Engl.*, 2008, **47**(32), 6052.
- H. Song, M. Dai, H. Song, X. Wan and X. Xu, *Appl. Catal., A*, 2013, **462–463**(27), 247.
- L. Song, S. Zhang and Q. Wei, *Catal. Commun.*, 2011, **12**(12), 1157.
- Q. Guan and L. Wei, *J. Catal.*, 2010, **271**(2), 413.
- R. H. Bowker, M. C. Smith, M. L. Pease, K. M. Slenkamp and L. Kovarik, *ACS Catal.*, 2011, **1**(8), 917.
- N. Dharmaraj, P. Prabu, S. Nagarajan, C. H. Kim, J. H. Park and H. Y. Kim, *Mater. Sci. Eng., B*, 2006, **128**(1), 111.
- S. V. Pol, V. G. Pol, I. Felner and A. Gedanken, *Eur. J. Inorg. Chem.*, 2007, 2089.
- J. C. D. Jesús, S. García and D. Dorante, *J. Anal. Appl. Pyrolysis*, 2018, **130**, 332.
- R. Wang and K. J. Smith, *Appl. Catal., A*, 2010, **380**(1), 149.

- 21 N. Chen, S. Gong and E. W. Qian, *Appl. Catal., B*, 2015, **174–175**, 253.
- 22 E. Kordouli, C. Kordulis, A. Lycourghiotis, R. Cole, P. T. Vasudevan, B. Pawelec and J. L. G. Fierro, *Mol. Catal.*, 2017, **441**, 209.
- 23 J. Wan-Kuen, S. Karthikeyan, M. A. Isaacs, A. F. Lee, K. Wilson, S. Seung-Ho, L. Jun-ho, K. Mo-Keun, P. Byung-Sik and G. Sekaran, *J. Taiwan Inst. Chem. Eng.*, 2017, **74**, 289.
- 24 H. Song, Q. Yu, N. Jiang, Z. J. Yan, T. Z. Hao and Z. D. Wang, *Res. Chem. Intermed.*, 2018, **44**(5), 3629.
- 25 H. Song, J. Gong, H. L. Song and F. Li, *Appl. Catal., A*, 2015, **505**, 267.
- 26 G. J. Shi, Y. Zhao, Y. Huang and J. Shen, *Chin. J. Catal.*, 2010, **31**, 961.
- 27 K. A. Layman and M. E. Bussell, *J. Phys. Chem. B*, 2004, **108**, 10930.
- 28 L. F. Feitosa, G. Berhault, D. Laurenti, T. E. Davies and V. T. da Silva, *J. Catal.*, 2016, **340**, 154.
- 29 T. I. Korányi, Z. Vít, D. G. Poduval, R. Ryoo, H. S. Kim and E. J. M. Hensen, *J. Catal.*, 2008, **253**, 119.
- 30 H. Song, J. Wang, Z. D. Wang, H. L. Song, F. Li and Z. S. Jin, *J. Catal.*, 2014, **311**, 257.
- 31 T. Kawai, K. K. Bando, Y. K. Lee, S. T. Oyama, W. J. Chun and K. Asakura, *J. Catal.*, 2006, **241**, 20.
- 32 A. E. Nelson, M. Sun and A. S. M. Junaid, *J. Catal.*, 2006, **241**, 180.
- 33 T. H. Zhu, H. Song, X. Y. Dai and H. L. Song, *Chin. J. Chem. Eng.*, 2017, **12**, 25.